Fourierization of the Legendre–Galerkin method and a new space–time spectral method

Jie Shen [a],[*],[1], Li-Lian Wang [b]

[a] *Department of Mathematics, Purdue University, West Lafayette, IN, 47907, USA*
[b] *Division of Mathematical Sciences, School of Physical & Mathematical Sciences, Nanyang Technological University, 637616 Singapore*

Available online 10 August 2006

Abstract

A set of Fourier-like basis functions is constructed for Legendre–Galerkin method for non-periodic boundary value problems and a new space–time spectral method is proposed. A complete error analysis is carried out for a linear parabolic equation and numerical results are presented for several typical linear and nonlinear equations.
© 2006 IMACS. Published by Elsevier B.V. All rights reserved.

1. Introduction

Spectral method, in the context of numerical schemes, was introduced and popularized by Orszag's pioneer work in the early seventies. The term "spectral" was probably originated from the fact that the trigonometric functions $\{e^{ikx}\}$ are the eigenfunctions of the Laplace operator with periodic boundary conditions. This fact and the availability of Fast Fourier Transform (FFT) are two main advantages of the Fourier spectral method. Thus, using Fourier series to solve PDEs, with principal differential operator being the Laplace operator (or its power) with periodic boundary conditions, results in very attractive numerical algorithms. However, for problems with rigid boundaries, the eigenfunctions of Laplace operator (with non-periodic boundary conditions), although easily available in regular domains, are no longer good candidates as basis functions due to the Gibbs phenomenon (cf. [6]). In such cases, it is well known that one should use the eigenfunctions of the singular Sturm–Liouville operator, i.e., Jacobi polynomials with a suitable pair of indexes, e.g., Legendre and Chebyshev polynomials. Although these orthogonal polynomials have been successfully used for numerical approximation of PDEs (cf. [6,3,7,2]), there are still many situations where one wishes a set of Fourier-like basis functions would be available for non-periodic problems. The first objective of this paper is to construct such Fourier-like basis functions for elliptic boundary value problems. More precisely, we present an efficient and stable algorithm to construct basis functions which are mutually orthogonal with respect to both the

---

L^2- and H^1-inner products. In particular, this set of basis functions is very convenient in developing efficient space–time spectral method which is the second topic of this paper.

Despite the fact that solutions of most time-dependent PDEs of current interest are much smoother in time than they are in space (except perhaps at $t = 0$ for parabolic-type equations), in most practical situations, high-order spectral methods in space are coupled with a low-order finite difference scheme in time, creating a mismatch in accuracy, and often resulting in a severe time step restriction which could be prohibitive for higher-order differential equations. Hence, it is plausible, for certain type of time-dependent PDEs, to use a spectral method for both space and time. We refer to [16] (see also [15,1] and the references therein) for an account on the rather limited activities in this area. It appears that the analysis for such space–time spectral methods are all restricted to periodic (in space) problems. Hence, the second objective of this paper is to present a new space–time spectral method based on a Legendre–Galerkin method in space and a dual-Petrov–Galerkin formulation in time. We also demonstrate that the use of Fourier-like basis functions in space may greatly simplify the implementation of the new space–time spectral method.

The rest of the paper is organized as follows. In the next section, we construct the Fourier-like basis functions. In Section 3, we propose the space–time spectral method and derive an optimal error estimate for a simple model problem. We present in Section 4 some illustrative numerical results. Some concluding remarks are given in the last section.

We now introduce some notations. Let ω be a positive weight function in a bounded domain Ω, and denote by $(u, v)_{\Omega,\omega} := \int_\Omega uv\omega \, d\Omega$ the inner product of $L^2_\omega(\Omega)$ whose norm is denoted by $\|\cdot\|_{\Omega,\omega}$. We use $H^m_\omega(\Omega)$ and $H^1_{0,\omega}(\Omega)$ to denote the usual weighted Sobolev spaces. For any Banach space X with norm $\|\cdot\|_X$, we define $L^2((a, b); X) = \{v: \int_a^b \|v\|^2_X \, dt < +\infty\}$. In cases where no confusion would arise, ω (if $\omega \equiv 1$) and Ω may be dropped from the notations. We denote by P_M the space of all polynomials of degree $\leqslant M$, and by c a generic positive constant independent of any function and of any discretization parameters. We use the expression $A \lesssim B$ to mean that $A \leqslant cB$.

2. Fourier-like basis functions for the Legendre–Galerkin method

Many physical problems are governed by PDEs of the form

$$u_t = \mathcal{L}u + \mathcal{N}(u, t), \tag{2.1}$$

where $\mathcal{L}$ and $\mathcal{N}$ are higher-order linear and lower-order nonlinear operators, respectively. Typical examples include the Allen–Cahn, Burgers, Navier–Stokes, nonlinear Schrödinger, Cahn–Hilliard and Kuramoto–Sivashinsky equations. To approximate such problems, high-order stable numerical schemes in space and time are desirable but are not easy to construct due to the combinations of nonlinearities and stiffness.

A suitable semi-discretization in space of (2.1) leads to the following ODE system

$$\mathbf{M}\bar{u}_t = \mathbf{L}\bar{u} + \mathbf{N}(\bar{u}, t), \tag{2.2}$$

where $\bar{u}$ is an unknown vector consisting of either expansion coefficients (in terms of basis functions of the approximation space) of the approximate solution or the nodal values of the approximate solution, and $\mathbf{M}$ and $\mathbf{L}$ are the mass and stiffness matrices, respectively.

In a recent work [10], Kassam and Trefethen compared and evaluated five high-order time-stepping methods, i.e., implicit–explicit, split step, integrating factor, sliders and exponential time-differencing, coupled with spatial discretizations using Fourier and Chebyshev collocation methods for problem (2.1) with periodic and non-periodic boundary conditions. As pointed out in [10], having diagonal mass and stiffness matrices is crucial in the implementation and analysis of some time-stepping schemes. In particular, the *sliders* method (cf. [5]), in which different schemes are used for "fast", "medium" and "slow" modes, is designed essentially for periodic problems. However, for non-periodic problems, the commonly-used basis functions in a spectral approximation lead to either a diagonal mass matrix (as in the collocation method) or a diagonal stiffness matrix (as in the Legendre–Galerkin method [12]) but not both. Therefore, many of the high-order, efficient time stepping schemes cannot be directly designed, so it is of interest to construct Fourier-like basis functions for spatial discretization of non-periodic problems.

To demonstrate the main idea, we consider the following one-dimensional problem

$$\partial_t u - \alpha \partial_x^2 u + \mathcal{N}(u, t) = 0, \quad x \in I := (-1, 1), \ t > 0,$$
$$u(x, 0) = u_0(x), \quad x \in \bar{I}, \tag{2.3}$$

with the boundary conditions

$$a_\pm u(\pm 1, t) + b_\pm u_x(\pm 1, t) = 0, \quad t \geqslant 0. \tag{2.4}$$

To ensure the well-posedness, we assume that the constants $a_\pm$ and $b_\pm$ satisfy the following conditions

$$\text{(i) } a_\pm \geqslant 0; \qquad \text{(ii) } a_-^2 + b_-^2 \neq 0, \quad a_- b_- \leqslant 0; \qquad \text{(iii) } a_+^2 + b_+^2 \neq 0, \quad a_+ b_+ \geqslant 0. \tag{2.5}$$

Hence, (2.4) includes in particular the Dirichlet ($a_\pm = 1$ and $b_\pm = 0$), the Neumann ($a_\pm = 0$ and $b_\pm = 1$), and the mixed boundary conditions ($a_- = b_+ = 0$ or $a_+ = b_- = 0$).

We define the approximation space as

$$V_M = \{v \in P_M : a_\pm v(\pm 1) + b_\pm v_x(\pm 1) = 0\}. \tag{2.6}$$

The semi-discrete Legendre–Galerkin approximation of (2.3)–(2.4) is to

$$\begin{cases} \text{Find } u_M(t) \in V_M \text{ such that} \\ (\partial_t u_M, v) - \alpha(\partial_x^2 u_M, v) + (\mathcal{N}(u_M, t), v) = 0, \quad \forall v \in V_M, \ t > 0. \end{cases} \tag{2.7}$$

It is shown in [13] that there exists a unique set $\{a_k, b_k\}$ such that

$$\gamma_k(x) = L_k(x) + a_k L_{k+1}(x) + b_k L_{k+2}(x) \in V_{k+2},$$

where $L_j(x)$ is the Legendre polynomial of degree j. Hence,

$$V_M = \text{span}\{\gamma_k : 0 \leqslant k \leqslant M - 2\}.$$

Using the properties of Legendre polynomials, one verifies readily that under this basis (with a proper scaling), the stiffness matrix $\mathbf{S}$ (with entries $s_{ij} = -(\gamma_j'', \gamma_i)$) is an identity matrix, and the mass matrix $\mathbf{M}$ (with entries $m_{ij} = (\gamma_j, \gamma_i)$) is a symmetric positive definite penta-diagonal matrix.

2.1. Fourier-like basis functions

We are now in a position to construct a new basis which leads to diagonal stiffness and mass matrices. The idea is to construct *discrete* eigenfunctions of the Laplace operator. Since the mass matrix $\mathbf{M}$ (associated with the basis $\{\gamma_j\}$) is a symmetric positive definite penta-diagonal matrix, its eigenpairs (all are real) can be easily computed. Let $\mathbf{E} = (e_{ij})_{i,j=0,\dots,M-2}$ be the matrix formed by the orthonormal eigenvectors of $\mathbf{M}$ and $\Lambda = \text{diag}(\lambda_i)$ be the diagonal matrix with main diagonal being the corresponding eigenvalues, i.e.,

$$\mathbf{M}\mathbf{E} = \mathbf{E}\Lambda, \qquad \mathbf{E}^t \mathbf{E} = \mathbf{I}_{M-1},$$

where $\mathbf{I}_{M-1}$ denotes the identity matrix of order $M-1$. Since the matrix $\mathbf{E}$ is nonsingular, the linear combinations

$$\phi_k(x) := \sum_{j=0}^{M-2} e_{jk} \gamma_j(x), \quad 0 \leqslant k \leqslant M - 2, \tag{2.8}$$

form a new basis of V_M satisfying

$$(\phi_l, \phi_i) = \sum_{k,j=0}^{M-2} e_{kl} e_{ji} (\gamma_k, \gamma_j) = \sum_{k,j=0}^{M-2} e_{ji} m_{jk} e_{kl} = (\mathbf{E}^T \mathbf{M} \mathbf{E})_{il} = \lambda_i \delta_{il},$$

$$-(\phi_l'', \phi_i) = -\sum_{k,j=0}^{M-2} e_{kl} e_{ji} (\gamma_k'', \gamma_j) = \sum_{k,j=0}^{M-2} e_{ji} \delta_{jk} e_{kl} = \delta_{il}, \tag{2.9}$$

where δ_{il} is the Kronecker symbol. In other words, the stiffness and mass matrices under this new basis $\{\phi_k\}_{k=0}^{M-2}$ are both diagonal. An immediate consequence of (2.9) is that

$$-(\phi_l'', \phi_i) = \lambda_l^{-1}(\phi_l, \phi_i)$$

which implies

$$-(\phi_l'', v) = \lambda_l^{-1}(\phi_l, v), \quad \forall v \in V_M. \tag{2.10}$$

Hence, $\{\phi_k\}_{k=0}^{M-2}$ are the (discrete) eigenfunctions of the Laplace operator in V_M, and can be referred to as *Fourier-like* basis functions.

The construction of the Fourier-like basis functions only involves finding all the eigenpairs of a symmetric positive definite penta-diagonal matrix (which, in the case of Dirichlet or Neumann boundary conditions, can be split up into two tri-diagonal matrices). Hence, this process is very efficient and stable. Note that it is also possible to construct such basis functions from a collocation approach by diagonalizing the derivative matrix, but such approach requires finding all the eigenpairs of a nonsymmetric full matrix which is more expensive and prone to large round-off errors.

2.2. Properties and applications of Fourier-like basis functions

Let us first look at the matrix form of (2.7) under the Fourier-like basis. Setting

$$u_M(x,t) = \sum_{j=0}^{M-2} \tilde{u}_j(t)\phi_j(x), \qquad \tilde{\mathbf{u}}(t) = (\tilde{u}_0, \tilde{u}_1, \ldots, \tilde{u}_{M-2})^t,$$

$$\tilde{f}_k(\tilde{\mathbf{u}}(t)) = (\mathcal{N}(u_M, t), \phi_k),$$

and taking $v = \phi_k$ in (2.7), we arrive at a system of nonlinear ODEs:

$$\lambda_k \tilde{u}_k'(t) + \alpha \tilde{u}_k(t) + \tilde{f}_k(\tilde{\mathbf{u}}(t)) = 0, \quad 0 \leqslant k \leqslant M - 2. \tag{2.11}$$

Note that this system is essentially the same as the Fourier approximation to (2.3) with a periodic boundary condition.

Among the many advantages of using Fourier-like basis functions are as follows.

- It provides a convenient separation of scales and would be very useful in developing multi-level spectral methods (cf. [4]). This separation also makes it possible to use the *sliders* time-stepping method (cf. [5,10]) for non-periodic problems.
- The exact solution of (2.11) can be formally expressed as

$$\tilde{u}_k(t) = \exp(-\alpha\lambda_k^{-1}t)\tilde{u}_k(0) - \int_0^t \exp(-\alpha\lambda_k^{-1}(t-s))\tilde{f}_k(\tilde{\mathbf{u}}(s))\,ds. \tag{2.12}$$

Since the principle linear operator can be integrated exactly as above, there is a wide variety of efficient and accurate ways to approximate the last integral in (2.12). In particular, the construction of high-order schemes for (2.3) (cf. formulas (1.3), (1.8) and (2.1)–(2.3) in [10]) becomes as efficient as the Fourier case.

- Multidimensional problems can be handled similarly using tensor product. For instance, one can build a more efficient elliptic solver using the Fourier-like basis functions. As an illustrative example, we consider the two-dimensional Poisson-type equation

$$\alpha u - \Delta u = f \quad \text{in } I \times I, \tag{2.13}$$

with the boundary conditions

$$a_\pm u(\pm 1, y) + b_\pm u_x(\pm 1, y) = 0, \qquad c_\pm u(x, \pm 1) + d_\pm u_y(x, \pm 1) = 0, \tag{2.14}$$

where the pairs $(a_\pm, b_\pm)$ and $(c_\pm, d_\pm)$ satisfy (2.4). Let $\{\phi_k(x), \lambda_k\}$ and $\{\psi_k(y), \mu_k\}$ be the discrete eigenfunctions and eigenvalues constructed above with the boundary conditions (2.14) in the x and y directions, respectively. Let us denote $L = (M, N)$ and define

$$V_L = \text{span}\{\phi_k(x)\psi_j(y): 0 \leqslant k \leqslant M - 2;\ 0 \leqslant j \leqslant N - 2\}. \tag{2.15}$$

Then, the Legendre–Galerkin method for (2.13) is to

$$\begin{cases} \text{Find } u_L \in V_L \text{ such that} \\ \alpha(u_L, v) - (\Delta u_L, v) = (f, v)_L, \quad \forall v \in V_L, \end{cases} \tag{2.16}$$

where $(\cdot,\cdot)_L$ are the discrete inner product based on the Gauss–Lobatto quadrature in $\Omega = I \times I$. Setting

$$u_L(x,y) = \sum_{k=0}^{M-2} \sum_{j=0}^{N-2} \tilde{u}_{kj} \phi_k(x) \psi_j(y), \qquad \tilde{f}_{kj} = (f, \phi_k \psi_j)_L.$$

It is easy to verify that the solution of (2.16) is given by:

$$\tilde{u}_{kj} = (\lambda_k \mu_j \alpha + \mu_j + \lambda_k)^{-1} \tilde{f}_{kj}. \tag{2.17}$$

Hence, this algorithm is even more efficient than that presented in [12] which was based on the basis functions $\{\gamma_k(x)\gamma_j(y)\}$.

- As we shall show in the forthcoming section, it leads to a robust spectral algorithm in space–time.

Remark 2.1. The procedure can be easily extended to Legendre–Galerkin (respectively dual-Petrov–Legendre–Galerkin [14]) method for one-dimensional fourth-order (respectively third-order) problems. More precisely, a set of Fourier-like basis functions leading to a diagonal "stiffness" matrix for the leading forth-order (respectively third-order) operator and a diagonal mass matrix can be constructed in the same fashion. However, how to design an efficient and stable process for diagonalizing the Stokes operator is still a challenging problem.

3. Space–time Legendre spectral method

In this section, we propose a new space–time spectral method based on Legendre–Galerkin method using Fourier-like bases in space and a dual-Petrov–Legendre–Galerkin formulation in time. We also describe its numerical implementation and carry out an error analysis for a model linear parabolic equation.

For simplicity of presentation, we consider once again (2.3), and shift the time interval to $I_t = (-1, 1)$:

$$\begin{aligned}
&\partial_t u - \alpha \partial_x^2 u + \mathcal{N}(u, t) = 0, \quad (x, t) \in \Omega := I_x \times I_t, \\
&u(\pm 1, t) = 0, \quad t \in \bar{I}_t, \\
&u(x, -1) = u_0(x), \quad x \in \bar{I}_x,
\end{aligned} \tag{3.1}$$

where $I_x = (-1, 1)$ and f, u_0 are given functions with $u_0(\pm 1) = 0$. Without loss of generality, we assume that $u_0 \equiv 0$, since inhomogeneous data can be handled easily by considering $v = u - u_0$.

Among the limited discussions on spectral method in time, Tal-Ezer [15] proposed a pseudo-spectral scheme in time for linear periodic parabolic equations. In [16], a space–time spectral scheme with a Legendre–tau method in time and Fourier method in space was introduced and analyzed for linear periodic problems.

For the Legendre–Galerkin method in space, we introduce the approximation space

$$V_M = \{u \in P_M: u(\pm 1) = 0\}. \tag{3.2}$$

Since (3.1) is a first-order equation in time, it is natural to use a dual-Petrov–Legendre–Galerkin method (cf. [14]). For this purpose, we define a pair of "dual" approximation spaces (in time):

$$S_N = \{u \in P_N: u(-1) = 0\}, \qquad S_N^* = \{u \in P_N: u(1) = 0\}. \tag{3.3}$$

Then, the new space–time spectral approximation of (3.1) is to

$$\begin{cases}
\text{Find } u_L := u_{MN} \in V_M \otimes S_N \text{ such that} \\
(\partial_t u_L, v)_\Omega + \alpha(\partial_x u_L, \partial_x v)_\Omega + (\mathcal{N}(u_L, t), v)_\Omega = 0, \quad \forall v \in V_M \otimes S_N^*.
\end{cases} \tag{3.4}$$

From the fact that for all $\phi \in S_N$, we have $\frac{1-t}{1+t} \phi \in S_N^*$, we find that the scheme (3.4) is equivalent to the following weighted Galerkin formulation:

$$\begin{cases}
\text{Find } u_L \in V_M \otimes S_N \text{ such that} \\
(\partial_t u_L, \phi)_{\Omega, \omega^{1,-1}} + \alpha(\partial_x u_L, \partial_x \phi)_{\Omega, \omega^{1,-1}} + (\mathcal{N}(u_L, t), \phi)_{\Omega, \omega^{1,-1}} = 0, \quad \forall \phi \in V_M \otimes S_N,
\end{cases} \tag{3.5}$$

where $\omega^{a,b}(t) = (1-t)^a (1+t)^b$ is the Jacobi weight function.

3.1. Implementation issues

We next discuss the numerical implementation of (3.4). We use the Fourier-like basis functions $\{\phi_k\}_{k=0}^{M-2}$ (cf. (2.8)) for V_M (in space). As for S_N and S_N^* (in time), we set

$$\psi_j(t) = L_j(t) + L_{j+1}(t), \qquad \psi_k^*(t) = L_k(t) - L_{k+1}(t). \tag{3.6}$$

Since $L_j(\pm 1) = (\pm 1)^j$, it is clear that $\{\psi_j\}_{j=0}^{N-1}$ (respectively $\{\psi_k^*\}_{k=0}^{N-1}$) forms a basis for S_N (respectively S_N^*). One verifies readily that

$$(\psi_j', \psi_i^*) = 2\delta_{ij}; \quad b_{ij} := (\psi_j, \psi_i^*) = 0, \quad \text{if } |i - j| > 1. \tag{3.7}$$

Setting $\mathbf{B} = (b_{ij})_{i,j=0,\dots,N-1}$ and

$$u_L(x, t) = \sum_{k=0}^{M-2} \sum_{j=0}^{N-1} \tilde{u}_{j,k} \phi_k(x) \psi_j(t), \qquad \tilde{n}_{j,k} = \big(\mathcal{N}(u_L, t), \phi_k(x)\psi_j(t)\big),$$

$$\mathbf{u}_k = (\tilde{u}_{0,k}, \tilde{u}_{1,k}, \dots, \tilde{u}_{N-2,k})^t, \qquad \mathbf{n}_k = (\tilde{n}_{0,k}, \tilde{n}_{1,k}, \dots, \tilde{n}_{N-2,k})^t, \tag{3.8}$$

the scheme (3.4) becomes

$$(2\lambda_k \mathbf{I}_{M-1} + \alpha \mathbf{B})\mathbf{u}_k + \mathbf{n}_k = 0, \quad k = 0, 1, \dots, M - 2. \tag{3.9}$$

If $\mathcal{N}(u, t)$ is nonlinear in u (as in most practical situations), (3.9) is a coupled nonlinear system of size $(M - 1)N$ and should be solved by using a suitable Newton-type iterative scheme such as the preconditioned Jacobian-free Newton–Krylov method (see [11] for a review on this subject). How to design an effective iterative approach capable of solving a large nonlinear systems resulted from the space–time spectral method is a very challenging task. Below are some of the strategies which could be used to improve the overall performance of the space–time spectral method.

- For many nonlinear equations, a suitable linear equation could be used as an effective preconditioner in the Jacobian-free Newton–Krylov method. For example, if we set $\mathcal{N}(u, t) = \beta u - f(x, t)$, then (3.9) is reduced to a sequence of tridiagonal systems:

  $$\big(2\lambda_k I_N + (\beta + \alpha\lambda_k)\mathbf{B}\big)\mathbf{u}_k = \mathbf{f}_k, \quad k = 0, 1, \dots, M - 2,$$

  with

  $$\tilde{f}_{j,k} = \big(f, \phi_k(x)\psi_j(t)\big)_L, \qquad \mathbf{f}_k = (\tilde{f}_{0,k}, \tilde{f}_{1,k}, \dots, \tilde{f}_{N-2,k})^t.$$

  This sequence of systems can be solved very efficiently, so it can be used as a preconditioner in the Jacobian-free Newton–Krylov method.
- The effectiveness of the Newton-type iteration relies heavily on obtaining a good initial guess. One can use, for example, a simple low-order numerical scheme to generate such an initial guess.
- One can also use the space–time spectral method as a post-processing scheme to obtain a highly accurate solution if needed.
- For large nonlinear problems, the space–time Legendre-spectral method should be implemented as a time marching scheme, i.e., we partition the time interval $[0, T]$ into K non-overlapping subintervals and apply the space–time spectral method on each subinterval sequentially with a relatively small N to reduce the computational complexity. The resulting algorithm is unconditionally stable and spectrally accurate in space and time (see Example 2 of the numerical results).

3.2. Error estimates

Since the full error analysis for the nonlinear system is beyond the scope of this paper, we shall only consider the analysis for a special case $\mathcal{N}(u, t) = \beta u - f$ where f is a given function. In this case, (3.4) becomes

$$(\partial_t u_L, v)_\Omega + \alpha(\partial_x u_L, \partial_x v)_\Omega + \beta(u_L, v)_\Omega = (f, v)_\Omega, \quad \forall v \in V_M \otimes S_N^*. \tag{3.10}$$

Let us first derive an *a priori* estimate on the approximate solution u_L.

Lemma 3.1. *If $\alpha > 0$, $\beta \geqslant 0$ and $f \in L^2_{\omega^{2,0}}(I_t; L^2(I_x))$, then the solution of* (3.10) *satisfies*

$$\|u_L\|_{\Omega, \omega^{0,-2}} + \sqrt{\alpha}\|\partial_x u_L\|_{\Omega, \omega^{-1,1}} + \sqrt{\beta}\|u_L\|_{\Omega, \omega^{1,-1}} \lesssim \|f\|_{\Omega, \omega^{2,0}}. \tag{3.11}$$

Proof. Taking $v = \frac{1-t}{1+t}u_L$ in (3.10), we derive the desired result by using the Cauchy–Schwartz inequality and the following identity:

$$(\partial_t u_L, u_L)_{\Omega, \omega^{1,-1}} = \frac{1}{2}\int_\Omega \left(\partial_t u_L^2\right)\omega^{1,-1}(t)\,\mathrm{d}t\,\mathrm{d}x = \int_\Omega u_L^2 \omega^{0,-2}(t)\,\mathrm{d}t\,\mathrm{d}x. \qquad \square \tag{3.12}$$

In the error analysis, we compare the numerical solution with a suitable orthogonal projection of the exact solution. The relevant orthogonal projection in space $\pi^{1,0}_M : H^1_0(I_x) \to V_M$ is defined by

$$\left(\left(\pi^{1,0}_M v - v\right)', \phi'\right)_{I_x} = 0, \quad \forall \phi \in V_M. \tag{3.13}$$

Lemma 3.2. *Let $\chi^a(x) := (1 - x^2)^a$. If $v \in H^1_0(I_x)$ and $\partial_x^k v \in L^2_{\chi^{k-1}}(I_x)$ with $1 \leqslant k \leqslant r$, then we have*

$$\left\|\partial_x^\mu\left(\pi^{1,0}_M v - v\right)\right\|_{I_x} \lesssim M^{\mu-r}\left\|\partial_x^r v\right\|_{I_x, \chi^{r-1}}, \quad \mu \leqslant r, \ \mu = 0, 1. \tag{3.14}$$

This estimate can be found, for instance, in [3], with an improvement of the weighted semi-norm in the upper bound given by [9].

We now introduce the orthogonal projection in time $P^{0,-1}_N : L^2_{\omega^{0,-1}}(I_t) \to S_N$, defined by

$$\left(P^{0,-1}_N v - v, \phi\right)_{I_t, \omega^{0,-1}} = 0, \quad \forall \phi \in S_N. \tag{3.15}$$

Defining

$$\widehat{H}^1(I_t) := \left\{u: u \in H^1(I_t) \cap L^2_{\omega^{0,-2}}(I_t)\right\},$$

one observes that for any $v \in \widehat{H}^1(I_t)$ and $\psi \in S^*_N$,

$$\left(\partial_t\left(P^{0,-1}_N v - v\right), \psi\right)_{I_t} = -\left(P^{0,-1}_N v - v, \omega^{0,1}\partial_t\psi\right)_{I_t, \omega^{0,-1}} = 0, \tag{3.16}$$

which follows from the fact $\omega^{0,1}\partial_t\psi \in S_N$ and the definition (3.15). As a special case of Theorem 1.1 in [8], we have the following approximation result.

Lemma 3.3. *If $v \in L^2_{\omega^{0,-1}}(I_t)$ and $\partial_t^k v \in L^2_{\omega^{k,k-1}}(I_t)$ for $1 \leqslant k \leqslant s$, then*

$$\left\|\partial_t^l\left(P^{0,-1}_N v - v\right)\right\|_{I_t, \omega^{l,l-1}} \lesssim N^{l-s}\left\|\partial_t^s v\right\|_{I_t, \omega^{s,s-1}}, \quad l \leqslant s, \ l = 0, 1. \tag{3.17}$$

For notational convenience, we denote by $A^r(\Omega)$ (respectively $B^s(\Omega)$) a function space consisting of measurable functions satisfying $\|u\|_{A^r(\Omega)} < +\infty$ (respectively $\|u\|_{B^s(\Omega)} < +\infty$), where for integers $r \geqslant 2$ and $s \geqslant 0$,

$$\|u\|_{A^r(\Omega)} = \left(\left\|\partial_t\partial_x^{r-1}u\right\|^2_{L^2_{\omega^{2,0}}(I_t; L^2_{\chi^{r-2}}(I_x))} + \left\|\partial_x^{r-1}u\right\|^2_{L^2_{\omega^{0,-1}}(I_t; L^2_{\chi^{r-2}}(I_x))} + \left\|\partial_x^r u\right\|^2_{L^2_{\omega^{1,-1}}(I_t; L^2_{\chi^{r-1}}(I_x))}\right)^{\frac{1}{2}};$$

$$\|u\|_{B^s(\Omega)} = \left(\left\|\partial_t^s\partial_x u\right\|^2_{L^2_{\omega^{s,s-1}}(I_t; L^2(I_x))} + \left\|\partial_t^s u\right\|^2_{L^2_{\omega^{s,s-1}}(I_t; L^2(I_x))}\right)^{\frac{1}{2}}.$$

With the aid of the previous lemmas, we are able to prove the following convergence result.

Theorem 3.1. *Let $\alpha > 0$ and $\beta \geqslant 0$, and let u, u_L be respectively the solutions of* (3.1) *(with $\mathcal{N}(u,t) = \beta u - f$) and* (3.10). *If $u \in L^2_{\omega^{1,-1}}(I_t; H^1_0(I_x)) \cap \widehat{H}^1(I_t; L^2(I_x)) \cap A^r(\Omega) \cap B^s(\Omega)$ with integers $r \geqslant 2$ and $s \geqslant 0$, then we have*

$$\|u - u_L\|_{\Omega, \omega^{0,-1}} + \left\|\partial_x(u - u_L)\right\|_{\Omega, \omega^{1,-1}} \lesssim N^{-s}\|u\|_{B^s(\Omega)} + M^{1-r}\|u\|_{A^r(\Omega)}. \tag{3.18}$$

Proof. Let us denote $\tilde{u}_L := P_N^{0,-1}\pi_M^{1,0}u = \pi_M^{1,0}P_N^{0,-1}u$ and $e_L := \tilde{u}_L - u_L$. Using (3.1) with $\mathcal{N}(u,t) = \beta u - f$ and (3.10) leads to

$$a(e_L, v) := (\partial_t e_L, v)_\Omega + \alpha(\partial_x e_L, \partial_x v)_\Omega + \beta(e_L, v)_\Omega$$
$$= \big(\partial_t(\tilde{u}_L - u), v\big)_\Omega + \alpha\big(\partial_x(\tilde{u}_L - u), \partial_x v\big)_\Omega + \beta(\tilde{u}_L - u, v)_\Omega,$$

for all $v \in V_M \otimes S_N^*$. Thanks to (3.13) and (3.16), the above equation can be simplified to

$$a(e_L, v) = \big(\partial_t(\pi_M^{1,0}u - u), v\big)_\Omega + \alpha\big(\partial_x(P_N^{0,-1}u - u), \partial_x v\big)_\Omega + \beta(\tilde{u}_L - u, v)_\Omega.$$

Taking $v = \frac{1-t}{1+t}e_L$ ($\in V_M \otimes S_N^*$) in the above equation and following the same lines as in the proof of Lemma 3.1, we derive that

$$\|e_L\|_{\Omega,\omega^{0,-2}} + \sqrt{\alpha}\|\partial_x e_L\|_{\Omega,\omega^{1,-1}} + \sqrt{\beta}\|e_L\|_{\Omega,\omega^{1,-1}}$$
$$\lesssim \big\|\partial_t(\pi_M^{1,0}u - u)\big\|_{\Omega,\omega^{2,0}} + \big\|\partial_x(P_N^{0,-1}u - u)\big\|_{\Omega,\omega^{1,-1}} + \|\tilde{u}_L - u\|_{\Omega,\omega^{1,-1}}. \tag{3.19}$$

The three terms at the right-hand side can be bounded by using Lemmas 3.2 and 3.3 as follows:

$$\big\|\partial_t(\pi_M^{1,0}u - u)\big\|_{\Omega,\omega^{2,0}} \lesssim M^{1-r}\big\|\partial_t\partial_x^{r-1}u\big\|_{L^2_{\omega^{2,0}}(I_t;L^2_{\chi^{r-2}}(I_x))},$$

$$\big\|\partial_x(P_N^{0,-1}u - u)\big\|_{\Omega,\omega^{1,-1}} \lesssim N^{-s}\big\|\partial_t^s\partial_x u\big\|_{L^2_{\omega^{s,s-1}}(I_t;L^2(I_x))},$$

$$\|\tilde{u}_L - u\|_{\Omega,\omega^{1,-1}} \lesssim \big\|P_N^{0,-1}(\pi_M^{1,0}u - u)\big\|_{\Omega,\omega^{0,-1}} + \big\|P_N^{0,-1}u - u\big\|_{\Omega,\omega^{0,-1}}$$
$$\lesssim \big\|\pi_M^{1,0}u - u\big\|_{\Omega,\omega^{0,-1}} + \big\|P_N^{0,-1}u - u\big\|_{\Omega,\omega^{0,-1}}$$
$$\lesssim M^{1-r}\big\|\partial_x^{r-1}u\big\|_{L^2_{\omega^{0,-1}}(I_t;L^2_{\chi^{r-2}}(I_x))} + N^{-s}\big\|\partial_t^s u\big\|_{L^2_{\omega^{s,s-1}}(I_t;L^2(I_x))}.$$

A combination of the above and (3.19) leads to

$$\|e_L\|_{\Omega,\omega^{0,-2}} + \sqrt{\alpha}\|\partial_x e_L\|_{\Omega,\omega^{1,-1}} \lesssim N^{-s}\|u\|_{B^s(\Omega)} + M^{1-r}\|u\|_{A^r(\Omega)}.$$

On the other hand, we have $u - u_L = u - \tilde{u}_L + e_L$. Hence, using Lemmas 3.2 and 3.3 again yields

$$\big\|\partial_x(u - \tilde{u}_L)\big\|_{\Omega,\omega^{1,-1}} \leqslant \big\|\partial_x\pi_M^{1,0}(P_N^{0,-1}u - u)\big\|_{\Omega,\omega^{1,-1}} + \big\|\partial_x(\pi_M^{1,0}u - u)\big\|_{\Omega,\omega^{1,-1}}$$
$$\lesssim \big\|\partial_x(P_N^{0,-1}u - u)\big\|_{\Omega,\omega^{1,-1}} + \big\|\partial_x(\pi_M^{1,0}u - u)\big\|_{\Omega,\omega^{1,-1}}$$
$$\lesssim N^{-s}\big\|\partial_t^s\partial_x u\big\|_{L^2_{\omega^{s,s-1}}(I_t;L^2(I_x))} + M^{1-r}\big\|\partial_x^r u\big\|_{L^2_{\omega^{1,-1}}(I_t;L^2_{\chi^{r-1}}(I_x))},$$

$$\|u - \tilde{u}_L\|_{\Omega,\omega^{0,-1}} \lesssim \big\|P_N^{0,-1}(\pi_M^{1,0}u - u)\big\|_{\Omega,\omega^{0,-1}} + \big\|P_N^{0,-1}u - u\big\|_{\Omega,\omega^{0,-1}}$$
$$\lesssim M^{1-r}\big\|\partial_x^{r-1}u\big\|_{L^2_{\omega^{0,-1}}(I_t;L^2_{\chi^{r-2}}(I_x))} + N^{-s}\big\|\partial_t^s u\big\|_{L^2_{\omega^{s,s-1}}(I_t;L^2(I_x))}.$$

Consequently, the desired result follows from the above estimates and the triangle inequality. $\quad\square$

Remark 3.1. We note that the above analysis is not restricted to the PDEs with the principal (spatial) operator being even-order elliptic operators. In fact, the same approach works when the principal (spatial) operator is odd-order (like in the KDV equation) *with suitable boundary conditions* (cf. [14]).

4. Numerical results

In this section, we present some numerical results obtained by the proposed space–time spectral method. Three examples: a linear problem (3.1) (with $\mathcal{N}(u,t) = \beta u - f$), a system of nonlinear ODEs and a nonlinear PDE, are considered below.
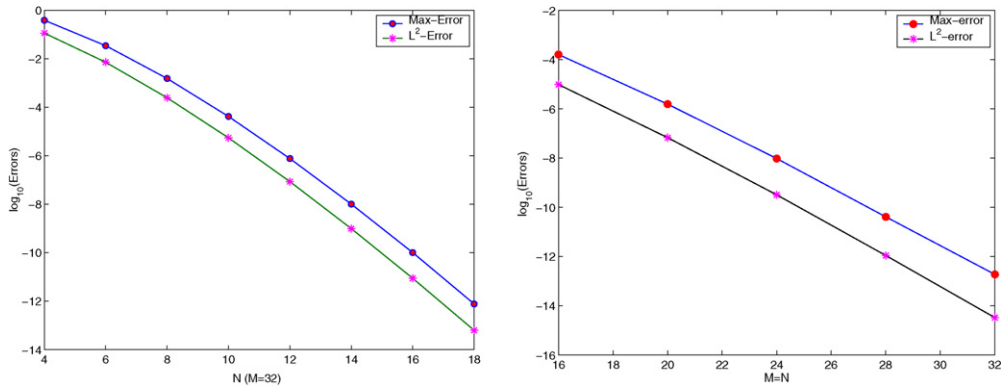
Fig. 1. Left: errors vs. N with $M = 32$; Right: errors vs. N with $M = N$.

Example 1. We consider Eq. (3.1) with $\mathcal{N}(u, t) = \beta u - f$, $\alpha = \beta = 1$, and the following exact solution

$$u(x, t) = \sin\left(t\left(1 - x^2\right)\pi\right), \quad (x, t) \in (-1, 1)^2.$$

To examine the error of time discretization, we fix $M = 32$ so that the spatial errors are negligible. In Fig. 1 (left), we plot the maximum point-wise errors and discrete L^2-errors in semi-log scale against various $N \leqslant 18$. The figure clearly indicates that the error decays like $O(e^{-cN})$. We note in particular that very high accuracy is achieved with quite small N for this smooth problem.

In Fig. 1 (right), we plot the errors vs. $M = N$ which also indicates an exponential convergence of order $O(e^{-cN})$.

Example 2. We consider the following Hamiltonian system

$$\frac{\mathrm{d}p}{\mathrm{d}t} = \partial_q H(p, q), \quad \frac{\mathrm{d}q}{\mathrm{d}t} = -\partial_p H(p, q), \quad t_0 < t \leqslant T,$$
$$p(t_0) = p_0, \qquad q(t_0) = q_0,$$
(4.1)

with the Hamiltonian

$$H(p, q) = a_1 q^2 + a_2 q^4 - a_3 p^2,$$
(4.2)

and the exact solution

$$H(p, q) = H_0 := H(p_0, q_0), \quad t \geqslant t_0.$$
(4.3)

For an efficient implementation, we partition the time interval $[t_0, T]$ into equidistant subintervals of length 2 by setting $K = [(T - t_0)/2]$, $t_k = t_0 + 2k$, $I_k = (t_k, t_{k+1})$ for $0 \leqslant k \leqslant K - 1$. Let $(\hat{p}^{k+1}(t), \hat{q}^{k+1}(t))$ be the numerical solution on the subinterval $\bar{I}_k$, which can be solved via the following system in I_k with the initial data $(\hat{p}^k(t_k), \hat{q}^k(t_k))$ (note: $(\hat{p}^0(t_0), \hat{q}^0(t_0)) = (p(t_0), q(t_0))$):

$$\begin{cases} \text{Find } (\hat{p}^{k+1}(t) - \hat{p}^k(t_k), \hat{q}^{k+1}(t) - \hat{q}^k(t_k)) \in (S_N, S_N) \text{ such that} \\ (\partial_t \hat{p}^{k+1}, v)_{I_k} = (\partial_p H(\hat{p}^{k+1}, \hat{q}^{k+1}), v)_{I_k}, \quad \forall v \in S_N^*, \\ (\partial_t \hat{q}^{k+1}, w)_{I_k} = -(\partial_q H(\hat{p}^{k+1}, \hat{q}^{k+1}), w)_{I_k}, \quad \forall w \in S_N^*, \end{cases}$$
(4.4)

sequentially for $0 \leqslant k \leqslant K - 1$. We then set the approximation solution as

$$\left.\left(\hat{p}(t), \hat{q}(t)\right)\right|_{t \in \bar{I}_k} = \left(\hat{p}^k(t), \hat{q}^k(t)\right), \quad 0 \leqslant k \leqslant K - 1.$$

In the following computations, we take $a_1 = 1/2$, $a_2 = -2/3$ and $a_3 = 1/2$ in (4.2), and suppose that the initial data is sitting on the curve

$$p(t_0) = 2a\cos(2t_0), \quad q(t_0) = a\sin(2t_0), \quad a = 1/4, \quad t_0 \in [0, \pi).$$
(4.5)

To solve the nonlinear system resulted from (4.4), we used a standard Newton iterative method with initial guesses computed by the Matlab function ode23. For a given absolute error tolerance $\epsilon = 10^{-6}$, only two or three iterations were needed for the following numerical tests.
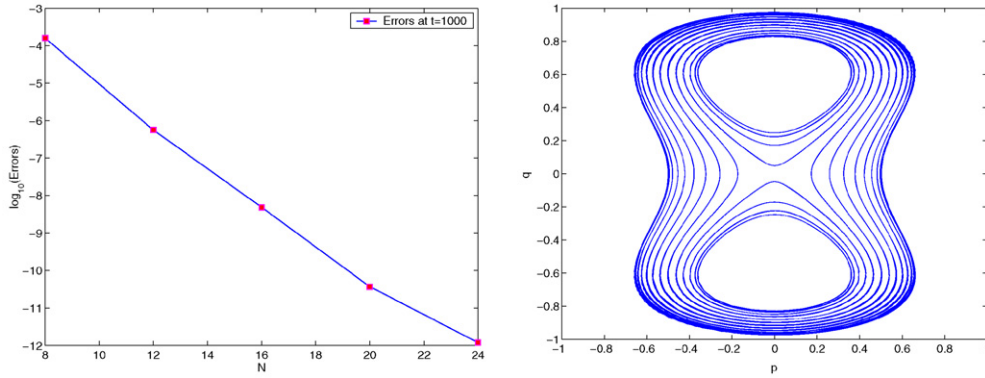
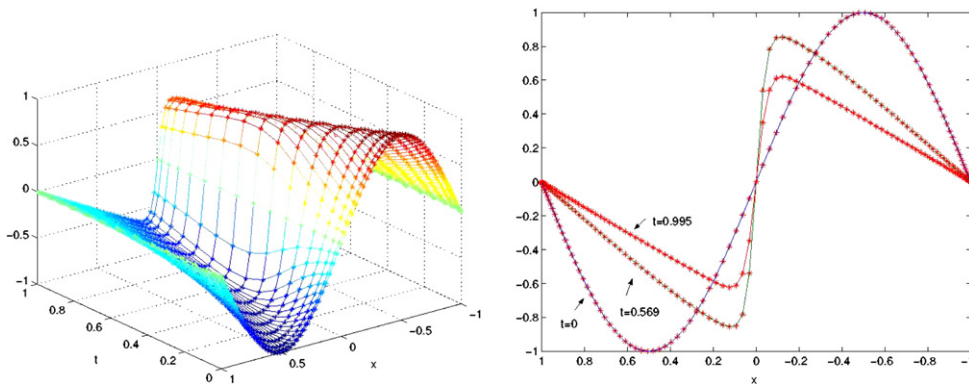Fig. 2. Left: error vs. N; Right: numerical solution with $N = 16$, $n = 500$.

Fig. 3. Left: u_e (solid line) vs. numerical solution (star-marker) with $\mu = 0.02$, $N = 16$, $M = 100$; Right: profiles of u_e (solid line) and the numerical solution (star-marker) at $t = 0, 0.569, 0.995$.

In Fig. 2 (left), we plot the maximum point-wise errors between $H(\hat{p}, \hat{q})$ and H_0 (with $t_0 = 0$ and $t = 1000$) against various N (number of points in each subinterval I_k), which indicates that spectral accuracy is preserved even for very large T.

In Fig. 2 (right), we plot in the phase plane the numerical solution $(\hat{p}, \hat{q})$ ($t \in [t_0, t_0 + 1000]$) obtained by the time marching scheme (4.4)–(4.5) with various initial data (i.e., different $t_0 \in [0, \pi)$), and with $N = 16$ points in each subinterval. Note that given $t_0 \in [0, \pi)$, the graph of the exact solution (4.3) ($t > t_0$) in the phase plane is a periodic orbit, and any two periodic orbits are disconnected. Thanks to the high accuracy of our scheme, the Hamiltonian H_0 is well preserved as indicated by the fact that for any given initial data, $(\hat{p}, \hat{q})$ stays on the same orbit for all $t \in [t_0, t_0 + 1000]$.

Example 3. In the last example, we examine the performance of our space–time spectral method for the Burgers equation

$$\partial_t u - \mu \partial_x^2 u + u \partial_x u = 0, \quad x \in (-1, 1), \quad t \in (0, T], \quad \mu > 0, \tag{4.6}$$

with the initial and boundary conditions

$$u(\pm 1, t) = 0, \quad t \in [0, T], \qquad u(x, 0) = -\sin(\pi x), \quad x \in [-1, 1]. \tag{4.7}$$

We note that for small value of viscosity μ, this problem will develop a thin internal layer which requires, in the absence of an adaptive strategy, a large number of spatial modes. We solve this nonlinear problem with our space–time spectral scheme coupled with a Newton iteration. Here, we take $\mu = 0.02$, $N = 16$ (mode in time), $M = 100$ (mode in space) and $T = 1$. For a comparison, we compute the "exact" solution $u_e(x, t)$ by using Crank–Nicolson in time and Legendre spectral method in space on very fine mesh with time step 10^{-4} and space mode 256. The

numerical solution (star-marker) against u_e (solid line) and their profiles at $t = 0, 0.569, 0.995$, are depicted in Fig. 3. It is clear that our scheme with a small N has produced a very accurate numerical result for this nonlinear PDE.

5. Concluding remarks

We presented in this paper a set of Fourier-like basis functions for the Legendre–Galerkin method and a new space–time spectral method.

The Fourier-like basis functions are discrete eigenfunctions of the Laplace operator and lead to diagonal mass and stiffness matrices. Hence, they behave essentially like Fourier series and are very convenient and efficient to use.

Our space–time spectral method is based on a dual-Petrov–Legendre–Galerkin method in time which has proved to be the natural formulation for first-order operators. We presented an optimal error analysis for model linear problems and elaborated on efficient implementations of our algorithm for nonlinear problems. As demonstrated by our numerical examples, the algorithm, being unconditionally stable and spectral accurate, can be used to solve, very accurately, nonlinear systems when combined with a suitable Newton–Krylov type iterative scheme.

It should be noted that the space–time spectral method is not meant as an replacement of the traditional time integration methods such as Runge–Kutta methods, rather, it is an alternative approach which could be very effective for certain problems where very high accuracy is needed over a long time interval. In a future work, we plan to investigate how to design robust and efficient iterative approaches capable of solving considerably large nonlinear systems using the space–time spectral method.

References

[1] P. Bar-Yoseph, E. Moses, U. Zrahia, A.L. Yarin, Space–time spectral element methods for one-dimensional nonlinear advection–diffusion problems, J. Comput. Phys. 119 (1) (1995) 62–74.

[2] J.P. Boyd, Chebyshev and Fourier Spectral Methods, second ed., Dover, Mineola, NY, 2001.

[3] C. Canuto, M.Y. Hussaini, A. Quarteroni, T.A. Zang, Spectral Methods in Fluid Dynamics, Springer, Berlin, 1987.

[4] T. Dubois, F. Jauberteau, R. Temam, Dynamic Multilevel Methods and the Numerical Simulation of Turbulence, Cambridge University Press, Cambridge, 1999.

[5] B. Fornberg, T.A. Driscoll, A fast spectral algorithm for nonlinear wave equations with linear dispersion, J. Comput. Phys. 155 (2) (1999) 456–467.

[6] D. Gottlieb, S.A. Orszag, Numerical Analysis of Spectral Methods: Theory and Applications, SIAM–CBMS, Philadelphia, PA, 1977.

[7] B. Guo, Spectral Methods and Their Applications, World Scientific, River Edge, NJ, 1998.

[8] B. Guo, J. Shen, L.-L. Wang, Optimal spectral-Galerkin methods using generalized Jacobi polynomials, J. Sci. Comput. 27 (2006) 305–322.

[9] B. Guo, L.-L. Wang, Jacobi approximations in non-uniformly Jacobi-weighted Sobolev spaces, J. Approx. Theor. 128 (2004) 1–41.

[10] A.-K. Kassam, L.N. Trefethen, Fourth-order time-stepping for stiff PDEs, SIAM J. Sci. Comput. 26 (4) (2005) 1214–1233 (electronic).

[11] D.A. Knoll, D.E. Keyes, Jacobian-free Newton–Krylov methods: a survey of approaches and applications, J. Comput. Phys. 193 (2) (2004) 357–397.

[12] J. Shen, Efficient spectral-Galerkin method I. Direct solvers for second- and fourth-order equations by using Legendre polynomials, SIAM J. Sci. Comput. 15 (1994) 1489–1505.

[13] J. Shen, Efficient Chebyshev–Legendre–Galerkin methods for elliptic problems, in: A.V. Ilin, R. Scott (Eds.), Proceedings of ICOSAHOM'95, Houston J. Math., 1996, pp. 233–240.

[14] J. Shen, A new dual-Petrov–Galerkin method for third and higher odd-order differential equations: application to the KDV equation, SIAM J. Numer. Anal. 41 (2003) 1595–1619.

[15] H. Tal-Ezer, Spectral methods in time for parabolic problems, SIAM J. Numer. Anal. 26 (1) (1989) 1–11.

[16] J.-g. Tang, H.-p. Ma, Single and multi-interval Legendre τ-methods in time for parabolic equations, Adv. Comput. Math. 17 (4) (2002) 349–367.